

A nested polyhedra model of isotropic MHD turbulence

Ö. D. Gürçan^{1,2}

¹ CNRS, Laboratoire de Physique des Plasmas, Ecole Polytechnique, Palaiseau and
² Sorbonne Universités, UPMC Univ Paris 06, Paris

A nested polyhedra model has been developed for magnetohydrodynamic (MHD) turbulence. Driving only the velocity field at large scales with random, divergence free forcing results in a clear, stationary $k^{-5/3}$ spectrum for both kinetic and magnetic energies. Since the model naturally effaces disparate scale interactions, does not have a guide field and avoids injecting any sign of helicity by random forcing, the resulting three dimensional k -spectrum is statistically isotropic. The strengths and weaknesses of the model are demonstrated by considering large or small magnetic Prandtl numbers. It was also observed that the time scale for the equipartition offset with those of the smallest scales shows a $k^{-1/2}$ scaling.

MHD turbulence has been studied in great detail in the past[1], in particular due to its relevance for space applications such as solar wind turbulence[2]. In the absence of external, or self generated mean magnetic fields, MHD turbulence tends to be isotropic[3]. While in nature mean magnetic fields abound, the statistically isotropic case, is interesting in its own right, which may be relevant when the background fields are sufficiently weak.

Nested polyhedra models were introduced recently as self-similar, spherically symmetric decimations of Fourier space using complete triangles in Navier-Stokes turbulence[4]. In these, the wave-vector domain is discretized using nested, alternating icosahedron dodecahedron pairs that are organized in such a way that wavevectors that are represented by the vertices of these objects always form complete triads between neighboring scales. They naturally respect the conservation laws of the original system and since the discretization is separated from the formulation of the equations, they are straightforward to develop for different systems. Here we show a similar model developed for MHD system of equations. The result is a model that describes the three dimensional spectral evolution of MHD turbulence, which in principle has the ability to represent anisotropy. Since there is no source of anisotropy however, the resulting turbulence is isotropic.

The Model- The nested polyhedra model of incompressible MHD equations can be written as:

$$\begin{aligned} \partial_t u_n^i + i\overline{M}_n^{ij\kappa} \sum_{\{n',n''\}=\mathbf{p}_n} \left(u_{n'}^{\kappa*} u_{n''}^{j*} - b_{n'}^{\kappa*} b_{n''}^{j*} \right) &= -\nu k_n^2 u_n^i \\ \partial_t b_n^i + i\delta M_n^{ij\kappa} \sum_{\{n',n''\}=\mathbf{p}_n} \left(u_{n'}^{\kappa*} b_{n''}^{j*} - b_{n'}^{\kappa*} u_{n''}^{j*} \right) &= -\eta k_n^2 b_n^i \end{aligned} \quad (1)$$

where $\overline{M}_n^{ij\kappa} = (M_n^{ij\kappa} + M_n^{i\kappa j})$, $\delta M_n^{ij\kappa} = (M_n^{ij\kappa} - M_n^{i\kappa j})$ and

$$M_n^{ij\kappa}(k) = k_n^\kappa \left[\delta_{ij} - \frac{k_n^i k_n^j}{k_n^2} \right].$$

Here the Einstein summation convention is used over repeated indices and the sums are computed over the set

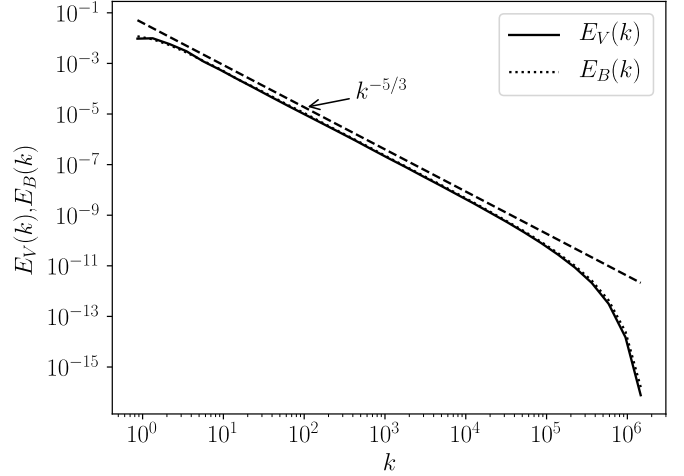


Figure 1. Reference case with $Pr_m = 1$, $\nu = 10^{-9}$, $N = 60$ and $h_f = 10^{-3}$ kinetic (solid line) and magnetic (dotted line) energy spectra, which follow perfectly the Kolmogorov's $k^{-5/3}$ spectrum. The case shown here is from a run up to $t = 500$ and the result is averaged over the polyhedra nodes and also from $t = 460$ to $t = 500$. In fact even an instantaneous spectrum is not so different when averaged over the polyhedra nodes as shown in Ref. 4 for Navier-Stokes.

of pairs \mathbf{p}_n that form a triad with the node n , which is determined by the geometry of nested polyhedra representation-independent from the equations- as described in detail in Ref. 4. Note that if the node belongs to the m th polyhedron in the nested hierarchy, it can form triads with pairs of nodes from neighboring polyhedra $m-2$, $m-1$, $m+1$ and $m+2$. Thus, the requirement of exact triads and the choice of the nodes on the vertices of nested polyhedra makes the interactions “local”, with a constant about 62% (i.e. $1/\varphi$ where $\varphi = (1 + \sqrt{5})/2$ is the golden ratio) for the ratio between the smallest to largest wavenumber of the interacting triad. Note that in this model this ratio is not a separate choice but imposed by the choice of the nested polyhedra geometry. The notation in (1) is such that n corresponds to the node number. The node numbers 0 to 5 belong to the first icosahedron (i.e. $m = 0$), while 6 to 15 correspond

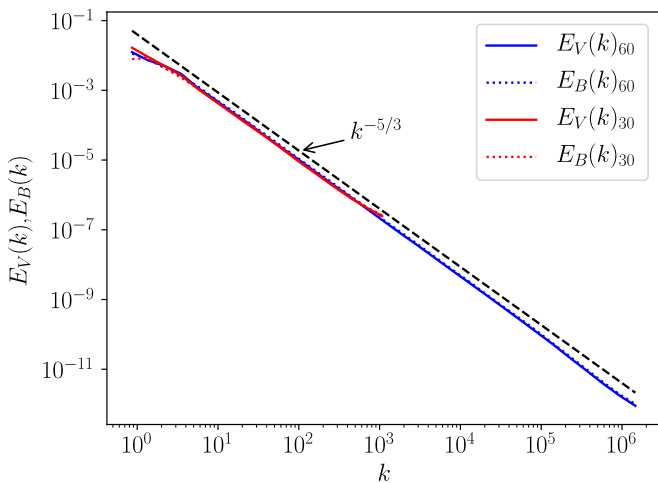


Figure 2. The high resolution case with $Pr_m = 1.0$, $\nu = 10^{-10}$, $N = 60$ and $h_f = 10^{-3}$ kinetic (solid blue line) and magnetic (dotted blue line) energies, together with the low resolution case with $N = 30$ and $\nu = 10^{-6}$ kinetic (solid red line) and magnetic (dotted red line) energies. The results are averaged over the nodes and from $t = 460$ to $t = 500$.

to the first dodecahedron (i.e. $m = 1$) and so on. This is because we only consider half of each polyhedron since $k_n^i \rightarrow -k_n^i$ gives $\{u_n^i, b_n^i\} \rightarrow \{u_n^{i*}, b_n^{i*}\}$ because of the condition that the fields $\mathbf{u}(\mathbf{x}, t)$ and $\mathbf{b}(\mathbf{x}, t)$ should be real. This means that in order to solve for N polyhedra (i.e. “shells”), $8N$ nodes have to be considered. Here n is the flattened node index number, which can be defined in terms of the polyhedron index number m and the node number ℓ within the polyhedron in consideration. While (1) written in such a way that the nonlinear terms are complex conjugates, in practice the interaction defines whether or not to complex conjugate each term. If the interaction pair in table X has a bar it means that the corresponding term in (1) is conjugated once more, which means it goes back to the unconjugated field. A hybrid python/fortran numerical implementation of the model using numpy[5] and f2py[6] can be found at http://github.com/gurcani/npm_mhd.

The model has some interesting features, such as no requirement for the existence of a dissipative range within the simulation domain simply by choosing the correct dissipation value. It also shows no sign of intermittency in the sense that it follows the $S_p(k_n) \sim k_n^{-p/3}$ scaling in the inertial range, where $S_p(k_n) = \left\langle \frac{1}{N_\ell} \sum_\ell \left(\sum_i |u_{n\ell}^i|^2 \right)^{p/2} \right\rangle$ and $\langle \cdot \rangle$ denotes time average.

Forcing- The model is implemented using an adaptive time step solver. Random forcing is implemented using a fixed time step $h_f \sim 10^{-3}$ which is larger than the maximum step size for the adaptive time stepping algorithm. In practice the forcing is applied *only on the velocity field*, for each node n of the polyhedra (i.e. shells) $m = 4$ and $m = 5$ as:

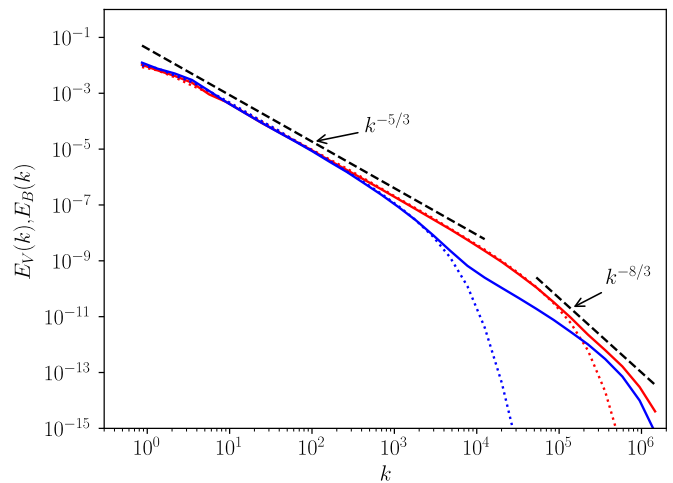


Figure 3. The case with $Pr_m = 10^{-2}$ (red) and $Pr_m = 10^{-4}$ (blue) with $\nu = 10^{-10}$, $N = 60$ and $h_f = 10^{-3}$ kinetic (solid line) and magnetic (dotted line) energy spectra. Note that the kinetic energy spectrum for $Pr_m = 10^{-2}$ seems to follow a $k^{-5/3}$ power law in the high- k range where the magnetic energy spectrum becomes dissipative. However when the Prandtl number is decreased further this is shown to be non-universal feature. The result is averaged over the nodes and from $t = 80$ to $t = 100$.

$$F_n^i = \left(\delta_{ij} - \frac{k_n^i k_n^j}{k_n^2} \right) \xi_j \quad (2)$$

where ξ_j is a vector random variable. The expression (2) guarantees that $k_n^i F_n^i = 0$ and that no helicity is injected. Indeed a preliminary attempt with $\xi_j = (1 + i) \times 10^{-2}$, a constant, which is a standard choice in shell models, lead to the development of large imbalances between $z^+ = u + b$ and $z^- = u - b$ asymptotically. Partly expected from the fact that such a forcing leads to strong correlation between u and b , which modifies the spectrum strongly[7]. Question of the relation between alignment and forcing and the relevance to real world MHD turbulence[8] is an important one. However, the simplest possible mathematical approach is to choose a forcing that eliminate velocity-magnetic field correlation[9]. This urged us to implement the random forcing discussed above, which removed the accumulation of imbalance. In a sense the imbalance should have been expected, since a constant forcing would lead to an accumulation of the alignment (or anti-alignment) between u and b .

Results- Three dimensional incompressible MHD spectra can be computed with little difficulty up to $N = 60$, where N is the total number of polyhedra in the nested polyhedra model. Starting from $k_0 = 1.0$, one gets $k_{max} = k_0 \varphi^{N/2}$. This means that a three dimensional wavenumber spectrum covering a range of more than 6 decades can easily be simulated with such a model. This is particularly useful if a clear identification of two or more different power laws are desired, such as the case with large or small magnetic Prandtl numbers

ℓ^m	$\mathbf{p}_{\ell,m} = \{\ell^{m-2}, \ell^{m-1}\}$	$\mathbf{p}_{\ell,m} = \{\ell^{m-1}, \ell^{m+1}\}$	$\mathbf{p}_{\ell,m} = \{\ell^{m+1}, \ell^{m+2}\}$
0	$\{(4, \bar{0}), (\bar{5}, \bar{1}), (\bar{1}, \bar{2}), (\bar{2}, \bar{3}), (\bar{3}, \bar{4})\}$	$\{(5, \bar{0}), (\bar{6}, \bar{1}), (\bar{7}, \bar{2}), (\bar{8}, \bar{3}), (\bar{9}, \bar{4})\}$	$\{(\bar{5}, \bar{4}), (\bar{6}, \bar{5}), (\bar{7}, \bar{1}), (\bar{8}, \bar{2}), (\bar{9}, \bar{3})\}$
1	$\{(3, \bar{0}), (4, \bar{4}), (\bar{5}, \bar{5}), (\bar{0}, \bar{7}), (\bar{2}, \bar{9})\}$	$\{(1, \bar{0}), (3, \bar{4}), (\bar{8}, \bar{5}), (\bar{2}, \bar{7}), (\bar{6}, \bar{9})\}$	$\{(\bar{1}, \bar{3}), (\bar{3}, \bar{4}), (\bar{8}, \bar{5}), (\bar{2}, \bar{0}), (\bar{6}, \bar{2})\}$
2	$\{(5, \bar{0}), (4, \bar{1}), (\bar{3}, \bar{5}), (\bar{1}, \bar{6}), (\bar{0}, \bar{8})\}$	$\{(4, \bar{0}), (2, \bar{1}), (\bar{7}, \bar{5}), (\bar{9}, \bar{6}), (\bar{3}, \bar{8})\}$	$\{(4, \bar{5}), (\bar{2}, \bar{4}), (\bar{7}, \bar{3}), (\bar{9}, \bar{1}), (\bar{3}, \bar{0})\}$
3	$\{(1, \bar{1}), (5, \bar{2}), (\bar{4}, \bar{6}), (\bar{2}, \bar{7}), (\bar{0}, \bar{9})\}$	$\{(0, \bar{1}), (3, \bar{2}), (\bar{8}, \bar{6}), (\bar{5}, \bar{7}), (\bar{4}, \bar{9})\}$	$\{(\bar{0}, \bar{1}), (\bar{3}, \bar{5}), (\bar{8}, \bar{4}), (\bar{5}, \bar{2}), (\bar{4}, \bar{0})\}$
4	$\{(\bar{0}, \bar{5}), (1, \bar{3}), (2, \bar{2}), (\bar{3}, \bar{8}), (\bar{5}, \bar{7})\}$	$\{(\bar{0}, \bar{5}), (4, \bar{3}), (1, \bar{2}), (\bar{6}, \bar{8}), (\bar{9}, \bar{7})\}$	$\{(\bar{0}, \bar{0}), (\bar{4}, \bar{1}), (\bar{1}, \bar{2}), (\bar{6}, \bar{3}), (\bar{9}, \bar{5})\}$
5	$\{(\bar{0}, \bar{6}), (\bar{1}, \bar{8}), (2, \bar{4}), (3, \bar{3}), (\bar{4}, \bar{9})\}$	$\{(\bar{1}, \bar{6}), (\bar{5}, \bar{8}), (0, \bar{4}), (2, \bar{3}), (\bar{7}, \bar{9})\}$	$\{(1, \bar{0}), (\bar{5}, \bar{1}), (\bar{0}, \bar{2}), (\bar{2}, \bar{3}), (\bar{7}, \bar{4})\}$

Table I. $n = 8m + \ell^m$ is interacting with $\mathbf{p}_n = \{n', n''\} = \{8m - 16 + \ell^{m-2}, 8m - 10 + \ell^{m-1}\}$, $\{8m - 10 + \ell^{m-1}, 8m + 6 + \ell^{m+1}\}$ and $\{8m + 6 + \ell^{m+1}, 8m + 16 + \ell^{m+2}\}$ for an even m (i.e. an icosahedron node) where ℓ^m , $\ell^{m\pm 1}$ and $\ell^{m\pm 2}$ are to be taken from the values given above, where if the integer value n' has a bar over it we replace $\{u_{n'}^{i*}, b_{n'}^{i*}\} \rightarrow \{u_{\bar{n}'}^i, b_{\bar{n}'}^i\}$ in the interaction term in (1).

$$Pr_m \equiv \nu/\eta.$$

The reference case corresponding to parameters $Pr_m = 1$, $\nu = 10^{-9}$, $N = 60$ and $h_f = 10^{-3}$ is shown in figure 1. Indeed this case is rather similar to a regularly discretized numerical simulation with the same parameters, except such a run with regular discretization would be hideously costly. One interesting aspect of the nested polyhedra models is that the dissipative range can be eliminated as shown in figure 2, in this case by taking $\nu = 10^{-10}$. Note that a smaller ν with the same N would lead to an increasing spectrum around the maximum k . This particular feature of the nested polyhedra model has the advantage that it does not need a subgrid model (such as large eddy simulation or LES) to push the dissipation range outside the simulation domain. Choosing the right value of dissipation is sufficient. A lower resolution case with $N = 30$ is also shown in figure 2. In fact even the case $N = 30$ is sufficiently resolved when the dissipative range is eliminated by the choice of ν . This is helpful because when one needs very good statistics such is the case for instance, when computing structure functions for intermittency corrections (typically runs up to $t = 25000$ may be needed) one can use lower resolution without losing any important features of the solution.

We have also considered different values of the magnetic Prandtl number Pr_m . The case $Pr_m = 10^{-2}$ is shown in blue in figure 3, representing the small magnetic Prandtl number behavior. We can see that while there appears to be a secondary range where the magnetic energy is dissipated and the kinetic energy seemingly displays a $k^{-8/3}$ power law scaling. However when the magnetic Prandtl number is decreased further to $Pr_m = 10^{-4}$, this behavior is lost and one recovers a $k^{-5/3}$ scaling also in this range as shown in figure 3. Note that, the model slows down when treating large or small Prandtl number cases, due to explicit treatment of linear terms. It is possible to alleviate this by using an implicit scheme or other more advance techniques such as exponential time integration schemes. Therefore the case with $Pr_m = 10^{-4}$ was integrated only up to $t = 100$

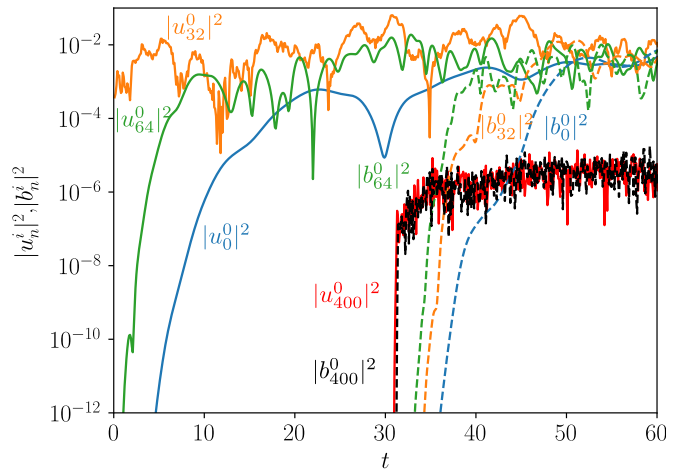


Figure 4. Different modes of the system as a function of time showing that the dynamo effect kicks in some time after the large scales are saturated. Here we can see the effects of random forcing on $|u_{32}^0|^2$, which then couples to other nodes.

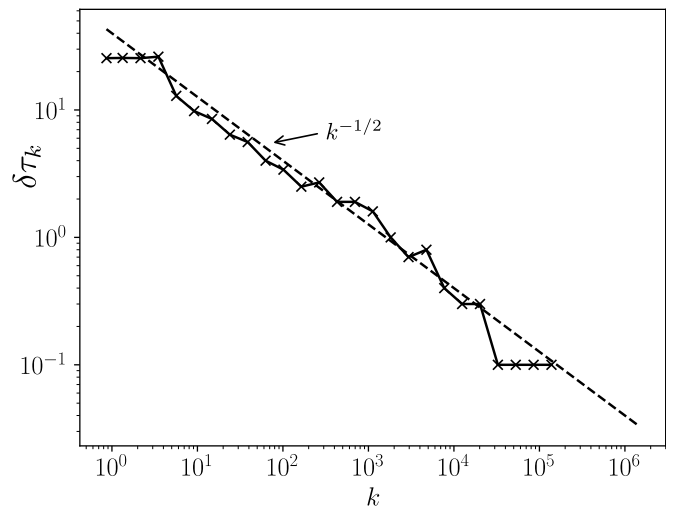


Figure 5. Equipartition time $\delta\tau_k = \tau_k - \tau_0$ with respect to the equipartition time of the smallest scales (i.e. τ_0) seems to roughly follow a $\delta\tau_k \propto k^{-1/2}$ scaling.

ℓ^m	$\mathbf{p}_{\ell,m} = \{\ell^{m-2}, \ell^{m-1}\}$	$\mathbf{p}_{\ell,m} = \{\ell^{m-1}, \ell^{m+1}\}$	$\mathbf{p}_{\ell,m} = \{\ell^{m+1}, \ell^{m+2}\}$
0	$\{(\bar{5}, \bar{0}), (\bar{1}, \bar{1}), (\bar{4}, \bar{2})\}$	$\{(4, \bar{0}), (\bar{3}, \bar{1}), (\bar{5}, \bar{2})\}$	$\{(\bar{4}, \bar{5}), (3, \bar{1}), (\bar{5}, \bar{4})\}$
1	$\{(\bar{6}, \bar{0}), (\bar{2}, \bar{2}), (\bar{0}, \bar{3})\}$	$\{(5, \bar{0}), (\bar{4}, \bar{2}), (\bar{1}, \bar{3})\}$	$\{(\bar{5}, \bar{6}), (\bar{4}, \bar{2}), (\bar{1}, \bar{0})\}$
2	$\{(\bar{7}, \bar{0}), (\bar{3}, \bar{3}), (\bar{1}, \bar{4})\}$	$\{(1, \bar{0}), (\bar{5}, \bar{3}), (\bar{2}, \bar{4})\}$	$\{(\bar{1}, \bar{7}), (\bar{5}, \bar{3}), (\bar{2}, \bar{1})\}$
3	$\{(\bar{8}, \bar{0}), (\bar{4}, \bar{4}), (\bar{2}, \bar{5})\}$	$\{(2, \bar{0}), (\bar{1}, \bar{4}), (\bar{3}, \bar{5})\}$	$\{(2, \bar{8}), (\bar{1}, \bar{4}), (\bar{3}, \bar{2})\}$
4	$\{(\bar{9}, \bar{0}), (\bar{3}, \bar{1}), (\bar{0}, \bar{5})\}$	$\{(3, \bar{0}), (\bar{4}, \bar{1}), (\bar{2}, \bar{5})\}$	$\{(\bar{3}, \bar{9}), (\bar{4}, \bar{3}), (\bar{2}, \bar{0})\}$
5	$\{(8, \bar{1}), (\bar{7}, \bar{2}), (\bar{0}, \bar{4})\}$	$\{(5, \bar{1}), (\bar{3}, \bar{2}), (\bar{0}, \bar{4})\}$	$\{(\bar{5}, \bar{8}), (\bar{3}, \bar{7}), (\bar{0}, \bar{0})\}$
6	$\{(9, \bar{2}), (\bar{8}, \bar{3}), (\bar{1}, \bar{5})\}$	$\{(1, \bar{2}), (\bar{4}, \bar{3}), (\bar{0}, \bar{5})\}$	$\{(\bar{1}, \bar{9}), (\bar{4}, \bar{8}), (\bar{0}, \bar{1})\}$
7	$\{(\bar{2}, \bar{1}), (\bar{5}, \bar{3}), (\bar{9}, \bar{4})\}$	$\{(\bar{0}, \bar{1}), (\bar{2}, \bar{3}), (\bar{5}, \bar{4})\}$	$\{(0, \bar{2}), (\bar{2}, \bar{5}), (\bar{5}, \bar{9})\}$
8	$\{(3, \bar{2}), (\bar{6}, \bar{4}), (\bar{5}, \bar{5})\}$	$\{(\bar{0}, \bar{2}), (\bar{3}, \bar{4}), (\bar{1}, \bar{5})\}$	$\{(0, \bar{3}), (\bar{3}, \bar{6}), (\bar{1}, \bar{5})\}$
9	$\{(6, \bar{1}), (\bar{4}, \bar{3}), (\bar{7}, \bar{5})\}$	$\{(2, \bar{1}), (\bar{0}, \bar{3}), (\bar{4}, \bar{5})\}$	$\{(\bar{2}, \bar{6}), (\bar{0}, \bar{4}), (\bar{4}, \bar{7})\}$

Table II. $n = 8m + \ell^m + 2$ is interacting with $\mathbf{p}_n = \{n', n''\} = \{8m - 14 + \ell^{m-2}, 8m - 4 + \ell^{m-1}\}$, $\{8m - 4 + \ell^{m-1}, 8m + 12 + \ell^{m+1}\}$ and $\{8m + 12 + \ell^{m+1}, 8m + 18 + \ell^{m+2}\}$ for an odd m (i.e. a dodecahedron node) where ℓ^m , $\ell^{m\pm 1}$ and $\ell^{m\pm 2}$ are to be picked from the values given above. As in table I, if the integer value n' has a bar over it we replace $\{u_{n'}^*, b_{n'}^*\} \rightarrow \{u_{n'}^i, b_{n'}^i\}$ in the interaction term in (1).

(saturated, but not very good statistics).

Dynamo- The simulations that are presented above, are all driven with a large scale random forcing of the velocity field. The resulting spectra however, present and almost perfect equipartition of kinetic and magnetic energies. When one studies how these final steady state spectra are established, one observes that it happens in stages. First, as the large scale kinetic energy reaches roughly its final maximum values a front in k -space of the kinetic energy appears, and fills the whole spectral domain. As this front reaches high- k end of the inertial range (roughly about $t \approx 30$ for the reference case above), equipartition between kinetic and magnetic energies gets established at high- k . Then another front (this time of the magnetic energy density) fills up the k -range moving towards smaller k . We can define the time it takes for the establishment of the equipartition τ_k which is a function of the wave-number k , which in general is a function of the initial conditions. The case of the very small seed initial conditions are shown in figure 5.

Conclusion- We show that a nested polyhedra model, obtained from “decimating” the wave-number space using self-similarly scaled nested, alternating icosahedra and dodecahedra, such that the wave-vectors that corresponds to two nodes of the system can combine to give a third one that also falls on a resolved node, can be used to model the MHD system of equations with no external magnetic field. In this model, the interactions are “local” in k -space (i.e. the ratio k_{n-2}/k_n of the smallest to the largest wavenumbers of the interacting triad is about 62%).

Considering isotropic MHD turbulence with no background magnetic field or rotation, and random large scale forcing on the velocity component, we find that the model

can display a clear Kolmogorov power law scaling of the form $k^{-5/3}$ over 6 decades in wave-number space with very good statistics, which allows considering large or small magnetic Prandtl number cases. Moreover, with a careful choice of the high- k dissipation, the apparent inertial range can extend all the way up to the end of the resolved range in k -space due to perfect self-similarity. Finally, since the random forcing was applied only on velocity, the magnetic energy spectrum gets established via the dynamo effect that starts from the small scales. It was observed that the time scale $\delta\tau_k = \tau_k - \tau_0$ for the equipartition, offset with the time of equipartition of the smallest scales shows a $k^{-1/2}$ scaling.

The author would like to thank W.-C. Müller, P. Morel, P. H. Diamond, R. Grappin and attendants of the *Festival de Théorie, Aix en Provence* in 2017.

-
- [1] D. Biskamp, *Magnetohydrodynamic Turbulence* (Cambridge University Press, 2003).
 - [2] O. Alexandrova, J. Saur, C. Lacombe, A. Mangeney, J. Mitchell, S. J. Schwartz, and P. Robert, *Phys. Rev. Lett.* **103**, 165003 (2009).
 - [3] W.-C. Müller and R. Grappin, *Phys. Rev. Lett.* **95**, 114502 (2005).
 - [4] O. D. Gürçan, *Phys. Rev. E* **95**, 063102 (2017).
 - [5] T. E. Oliphant, *Computing in Science Engineering* **9**, 10 (2007).
 - [6] P. Peterson, *International Journal of Computational Science and Engineering* **4**, 296 (2009).
 - [7] R. Grappin, J. Leorat, and A. Pouquet, *Astronomy and Astrophysics* **126**, 51 (1983).
 - [8] S. Boldyrev, *Phys. Rev. Lett.* **96**, 115002 (2006).
 - [9] M. E. McKay, M. Linkmann, D. Clark, A. A. Chalupa, and A. Berera, *Phys. Rev. Fluids* **2**, 114604 (2017).